Preparation, Solution Behavior, and Solid-State Structures of $(1,3\text{-}R_2C_5H_3)_2UX_2$, Where R Is CMe_3 or $SiMe_3$ and X Is a One-Electron Ligand

Wayne W. Lukens, Jr., Sharon M. Beshouri, Laura L. Blosch, Anthony L. Stuart, and Richard A. Andersen*

Chemistry Department and Chemical Sciences Division of Lawrence Berkeley Laboratory, University of California, Berkeley, California 94720

Received July 14, 1998

High-yield preparations of the uranium metallocenes $[1,3\text{-}(Me_3Si)_2C_5H_3]_2UCl_2$ (Cp''_2UCl_2) and $[1,3\text{-}(Me_3C)_2C_5H_3]_2UCl_2$ ($Cp^{\ddagger}_2UCl_2$) have been developed from the reaction of UCl_4 and the corresponding magnesocenes Cp''_2Mg and $Cp^{\ddagger}_2Mg$ in diethyl ether. The chloride ligands can be exchanged with either Me_3SiBr or Me_3SiI to give the uranium metallocene bromides or iodides. The fluorides were prepared by the reaction of $BF_3{\cdot}OEt_2$ with $Cp''_2U(NMe)_2$, $Cp^{\ddagger}_2U(OMe)_2$, or $Cp^{\ddagger}_2UMe_2$. The crystal structures of Cp''_2UCl_2, $Cp^{\ddagger}_2UCl_2$, Cp''_2UMe_2, $Cp^{\ddagger}_2UF_2$, and dimeric $(Cp''_2UF_2)_2$ are reported. The idealized symmetry of the monomers Cp''_2UX_2 and $Cp^{\ddagger}_2UCl_2$ is C_{2v} when X is F, Cl, or Br and C_2 when X is I or Me; in the dimer, the idealized symmetry is C_i. This preference is rationalized by intramolecular and intermolecular steric effects. The solution ring conformations and intramolecular exchange processes have been studied by variable-temperature ^1H NMR spectroscopy. In all cases, the low-temperature limiting spectra are consistent with the idealized symmetry observed in the solid state.

Introduction

The metallocene chemistry of tetravalent uranium has been dominated by two starting materials: Cp_3UCl[1−4] and $Cp^*_2UCl_2$,[5−8] where Cp* is Me_5C_5. The bulky pentamethylcyclopentadienyl ligand was developed to prevent ligand redistribution reactions, a feature that dominates the solution chemistry of unsubstituted f-block metallocenes. For example, neither Cp_2UCl_2 nor $Cp^*(Cp)UCl_2$ can be isolated due to the redistribution of their ligands in solution.[9−11] Redistribution also dominates the solution behavior of monosubstituted cyclopentadienyl ligands since $(RC_5H_4)_2UCl_2$, where R = $SiMe_3$ or CMe_3, cannot be isolated. In contrast, the crystal structure of $Cp^*_2UCl_2$ shows that it is a normal, monomeric bent metallocene.[12] This complex shows no tendency to undergo ligand redistribution to form the unknown Cp^*_3UCl.

A few disubstituted cyclopentadienylmetallocenes of the type Cp''_2UX_2, where Cp″ is $1,3\text{-}(Me_3Si)_2C_5H_3$, have been prepared and shown to be typical bent metallocenes by crystallography.[13−15] These complexes and the related $Cp^{\ddagger}_2UX_2$ complexes, where $Cp^{\ddagger}$ is $1,3\text{-}(Me_3C)_2C_5H_3$, should be ideal for studying ring conformations in the solid state and ring rotation and intermolecular ligand exchange in solution, since the R groups in $(R_2C_5H_3)_2U(X)(Y)$ are diastereotopic. In addition, Lappert has shown that these U(IV) metallocenes are ideal synthons for dimeric trivalent uranium metallocenes in which similar dynamic processes can be studied. In this paper we describe the synthesis and properties of Cp''_2UX_2 and $Cp^{\ddagger}_2UX_2$, and in an accompanying paper we describe the solution behavior of their U(III) reduction products.

Results and Discussion

Synthesis and Physical Properties. The starting metallocenes, Cp''_2UCl_2 and $Cp^{\ddagger}_2UCl_2$, were prepared by the reaction of UCl_4 with Cp''_2Mg[16] or $Cp^{\ddagger}_2Mg$ in diethyl ether, followed by crystallization from hexane

* To whom correspondence should be addressed at the Chemistry Department, University of California.

(1) Reynolds, L. T.; Wilkinson, G. *J. Inorg. Nucl. Chem.* **1956**, *2*, 246−253.
(2) Kanellakopolous, B. In *Organometallics of the f-Elements*; Marks, T. J., Fischer, R. D., Eds.; D. Reidel: Dordrecht, Holland, 1978; pp 1−36.
(3) Fischer, R. D. In *Organometallics of the f-Elements*; Marks, T. J., Fischer, R. D., Eds.; D. Reidel: Dordrecht, Holland, 1978; p 337.
(4) Marks, T. J. *Prog. Inorg. Chem.* **1979**, *25*, 223.
(5) Manriquez, J. M.; Fagan, P. J.; Marks, T. J. *J. Am. Chem. Soc.* **1978**, *100*, 3939.
(6) Fagan, P. J.; Manriquez, J. M.; Maatta, E. A.; Seyam, A. M.; Marks, T. J. *J. Am. Chem. Soc.* **1981**, *103*, 6650−6667.
(7) Marks, T. J.; Day, V. W. In *Fundamental and Technological Aspects of Organo-f-Element Chemistry*; Marks, T. J., Fragala, I. L., Eds.; D. Reidel: Dordrecht, Holland, 1985; pp 115−157.
(8) Fischer, R. D. In *Fundamental and Technological Aspects of Organo-f-Element Chemistry*; Marks, T. J., Fragala, I. L., Eds.; D. Reidel: Dordrecht, Holland, 1985; p 277.
(9) Ernst, R. D.; Kennelly, W. J.; Day, C. S.; Day, V. W.; Marks, T. J. *J. Am. Chem. Soc.* **1979**, *101*, 2656.
(10) Dormond, A. *J. Organomet. Chem.* **1981**, *256*, 47.
(11) Dormond, A.; Duval-Huet, C.; Tirouflet *J. Organomet. Chem.* **1981**, *209*, 341.
(12) Spirlet, M. R.; Rebizant, J.; Apostolidis, C.; Kanellakopolus, B. *Acta Crystallogr.* **1992**, *C48*, 2135.
(13) Hitchcock, P. B.; Lappert, M. F.; Singh, A.; Taylor, R. G.; Brown, D. *J. Chem. Soc., Chem. Commun.* **1983**, 561.
(14) Blake, P. C.; Lappert, M. F.; Taylor, R. G.; Atwood, J. L.; Hunter, W. E.; Zhang, H. *J. Chem. Soc., Chem. Commun.* **1986**, 1394−1395.
(15) Blake, P. C.; Lappert, M. F.; Taylor, R. G. *Inorg. Synth.* **1990,** *27*, 172.
(16) Duff, A. W.; Hitchcock, P. B.; Lappert, M. F.; Taylor, R. G.; Segal, J. A. *J. Organomet. Chem.* **1985**, *293*, 271−283.

10.1021/om9805988 CCC: $18.00
Publication on Web 03/04/1999

Table 1. ^{1}H NMR Chemical Shifts of the U(IV) Metallocene Complexes[a]

	$\delta(Me_3X)$ (X = C, Si)	$\delta(a_2)$	δ(b)	δ(other protons)	$\delta_b + \delta_{a_2}$
$Cp^{\ddagger}_2UF_2$	−1.38 (24)	−16.55 (36)	−9.61 (30)		−26.2
$Cp^{\ddagger}_2UCl_2$	0.31 (5)	−40.91 (14)	97.36 (15)		56.5
$Cp^{\ddagger}_2UBr_2$	1.54 (15)	−43.85 (45)	105.56 (38)		61.7
$Cp^{\ddagger}_2UI_2$	3.69 (13)	−46.20 (43)	108.31 (64)		62.1
Cp''_2UF_2	−0.76 (2)	−14.61 (9)	−16.14 (13)		−30.7
Cp''_2UCl_2	−2.60 (5)	−34.24 (15)	90.46 (24)		56.2
Cp''_2UBr_2	−1.60 (8)	−36.23 (24)	98.29 (30)		62.1
Cp''_2UI_2	−0.12 (10)	−37.80 (60)	101.30 (60)		63.5
$Cp^{\ddagger}_2UMe_2$	−0.64 (6)	−39.02 (9)	18.18 (12)	−35.43 (14) [U−Me]	−20.8
Cp''_2UMe_2	−1.19 (3)	−28.42 (6)	7.61 (6)	−21.03 (7) [U−Me]	−20.8
$Cp^{\ddagger}_2U(Me)Cl$	3.46 (4)	−29.52 (12)	55.6 (12)	−52.42 (20) [U−Me]	20.0
	−3.82 (4)	−41.78 (10)			
$Cp''_2U(Me)Cl$	0.14 (3)	−25.62 (8)	46.82 (9)	−49.90 (20) [U−Me]	18.0
	−3.77 (3)	−32.00 (8)			
$Cp^{\ddagger}_2U(OMe)_2$	−1.56 (5)	−25.89 (8)	−9.02 (5)	37.12 (5) [U−OMe]	−34.9
$Cp''_2U(OMe)_2$	−1.24 (3)	−25.09 (4)	−10.75 (4)	46.32 (4) [U−OMe]	−35.8
$Cp''_2U(NMe_2)_2$	0.07 (3)	−10.82 (11)	−5.70 (6)	9.82 (5) [U−NMe_2]	−16.5

[a] The chemical shifts are expressed in δ units with $\delta > 0$ to high field in C_6D_6 or C_7D_8 at 30 °C. The values in parentheses are the full widths at half-maximum (Hz).

as gold or dark red needles, respectively, in yields from 50 to 80%. Cp''_2UCl_2 was prepared previously by the reaction of Cp″Li and UCl_4 in tetrahydrofuran (thf).[15] Surprisingly, the reaction of Cp''_2Mg with UCl_4 works very poorly in tetrahydrofuran, presumably due to the formation of $Cp''UCl_3(thf)_2$. The magnesocenes were used rather than the alkali-metal cyclopentadienyl reagents since the magnesocenes are easily purified by crystallization from hexane or by sublimation and since the magnesium reagents can be isolated as pure materials, enabling accurate control of stoichiometry. The chloride ligands in either Cp''_2UCl_2 or $Cp^{\ddagger}_2UCl_2$ can be metathetically exchanged using commercially available Me_3SiX to give Cp''_2UX_2 or $Cp^{\ddagger}_2UX_2$ in good yield, where X is Br or I.[17] This method is more convenient than the previous use of BX_3 to prepare Cp''_2UX_2 (X = Br, I), since Me_3SiX is easier to handle and use.[15] All of the dihalide complexes are soluble in hexane, from which they were crystallized. Each gives a monomeric molecular ion in its mass spectrum. All of the Cp''_2UX_2 complexes are orange, while all of the $Cp^{\ddagger}_2UX_2$ complexes are red. All of the complexes melt cleanly; the $Cp^{\ddagger}$ derivatives melt ca. 20 °C higher than those of Cp″.

The fluorides were prepared by the method used to prepare Cp_2ZrF_2, viz., exchange with $BF_3{\cdot}OEt_2$.[18] The Cp″ derivative was prepared by the reaction between $Cp''_2U(NMe_2)_2$ and 2 equiv of $BF_3{\cdot}OEt_2$, and $Cp^{\ddagger}_2UF_2$ was prepared from $Cp^{\ddagger}_2UMe_2$ or $Cp^{\ddagger}_2U(OMe)_2$ and $BF_3{\cdot}OEt_2$. Both fluorides are hexane-soluble, but $Cp^{\ddagger}_2UF_2$ is significantly less soluble. Curiously, the colors of the fluorides are different from those of the other halides; Cp''_2UF_2 is dark green while $Cp^{\ddagger}_2UF_2$ is mustard yellow. The metallocene fluorides give monomeric molecular ions in their mass spectra.

The chloride ligands can also be sequentially replaced with methyl groups, as observed previously in $Cp^*_2UCl_2$ chemistry.[6] One equivalent of MeLi gives the methyl chloride complexes, isolated as orange-red crystals from hexane. Two equivalents of MeLi gives the highly soluble dimethyl complexes, which again may be isolated by crystallization from hexane. The dimethyl complexes yield M − Me ions in their mass spectra, but the methyl chloride complexes give molecular ions resulting from the redistribution of the methyl and chloride ligands. The bis(dimethylamide) complex $Cp''_2U(NMe_2)_2$ was obtained by metathesis using $LiNMe_2$ in tetrahydrofuran followed by crystallization from hexane.[19] The methoxides were obtained similarly using KOMe and are very soluble in hexane. Both methoxides give monomeric molecular ions in their mass spectra. Curiously, like the difluorides, the colors of the methoxides differ from the dihalides; $Cp''_2U(OMe)_2$ is purple, and $Cp^{\ddagger}_2U(OMe)_2$ is green.

The proton NMR chemical shifts at 30 °C of the U(IV) bent metallocenes are listed in Table 1. The resonances for all of the chemically inequivalent protons are observed, and the line widths of the Me_3C or Me_3Si hydrogens are between 5 and 15 Hz, generally less than those of the a_2- and b-methine protons on the cyclopentadienyl ring, the widths of which range from 5 to 60 Hz. The chemical shifts of the resonances strongly depend on the identity of X. In the dihalide compounds of the Me_3C and Me_3Si series, the chemical shifts of the a_2-protons move upfield ($\delta < 0$) by 20−30 ppm as X varies from iodide to fluoride. However, the chemical shifts of the b-protons move downfield ($\delta > 0$) as X changes from iodide to fluoride with a much larger change of about 100 ppm. The average in these two shifts may be conveniently expressed in the parameter $\Delta = \delta(b) + \delta(a_2)$, which reflects the net shift of the averaged ring C−H protons in the Me_3C- and Me_3Si-substituted metallocenes. The net shift decreases in the order I > Br > Cl > F, and the ring protons experience a net shielding (upfield shift) of 88 ppm (Me_3C) and 94 ppm (Me_3Si) upon changing from X = I to X = F; this is not a trivial shift. The change in the shift of the Me_3C or Me_3Si resonance is small (5 ppm or less) and does not vary systematically with the identity of X.

A related, though less extensive, correlation has been noted by Fisher in the Cp_3UX series.[3] In these compounds, the averaged Cp proton chemical shift moves upfield by ca. 7 ppm as X is changed from Cl to F. Fisher also observed that δ(Cp) moves upfield when X is Et_2N and EtO in the order Cl > F > NEt_2 > OEt. This order was suggested to result from ligand−metal π-bonding

(17) Andersen, R. A. *Inorg. Nucl. Chem. Lett.* **1980**, *16*, 31.
(18) Druce, P. M.; Kingston, B. M.; Lappert, M. F.; Spalding, T. R.; Srivastava, R. C. *J. Chem. Soc. A* **1969**, 2106−2110.
(19) Blake, P. C.; Lappert, M. F.; Taylor, R. G.; Atwood, J. L.; Zhang, H. *Inorg. Chim. Acta* **1987**, *129*, 12−20.

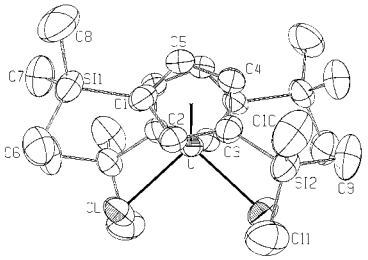

Figure 1. ORTEP drawing of Cp''_2UCl_2 with 50% thermal ellipsoids.

with the better π-donors causing greater shielding of the Cp hydrogen atoms. It is tempting to offer a similar rationalization for the dihalides reported here, since the value of Δ moves upfield with increasing π-donor ability of X. To allow a closer comparison of the bent metallocene values with those of Cp_3UX, the bent metallocenes with X = NMe_2 and MeO were prepared. As shown in Table 1, for these bent metallocenes, the Δ values move upfield in the order $Cl \gg Me_2N > F > OMe$. These data are consistent with Fisher's π-bonding hypothesis, although the ordering is slightly different in the two classes of complexes.

The Δ values for the dimethyl compounds lie between those of the difluorides and the dichlorides, as expected if chloride is reasonably assumed to be a poor π-donor. Further, in the mixed methyl−chloro species, the Δ values are additive; the observed Δ values are nearly the geometric mean of the dimethyl and dichloro values.

Table 1 clearly shows that the average room-temperature ^{1}H NMR chemical shifts are very sensitive to the nature of the X ligand, presumably due to changes in the bonding of X to the metallocene fragment. A postulate of π-bonding is offered without proof as a reasonable explanation for these trends. The origin of the isotropic chemical shifts in uranium compounds is determined by contact and dipolar contributions, and separating these contributions is very difficult, as previously noted by Fischer. However, the chemical shifts are nonetheless dependent upon the ligands and therefore diagnostic of differences in U−X bonding. The variable-temperature data will be discussed after the solid-state crystal structures are described, since the variable-temperature data cannot be understood without knowing the idealized molecular symmetry.

Crystal Structures. To determine whether the molecular structures of the complexes containing the postulated strong π-donor ligands are different from those with weak π-donor ligands, a representative series was crystallographically characterized. The molecular structures of Cp''_2UCl_2, $Cp^{\ddagger}_2UCl_2$, Cp''_2UMe_2, and $Cp^{\ddagger}_2UF_2$ are shown in Figures 1−4. The important distances and angles in these complexes are given in Table 2. In the solid state, Cp''_2UCl_2 has crystallographic C_2 symmetry with staggered cyclopentadienyl ligands. The bulky $SiMe_3$ groups are nearly eclipsed, and the Cp″ ligands point toward the front of the metallocene wedge (the front of the Cp″ ligand is defined by the unique b-hydrogen atom located between the R groups of the Cp″ ring). The ring conformations in $Cp^{\ddagger}_2UCl_2$ and $Cp^{\ddagger}_2UF_2$ are similar. All three compounds have similar X−U−X angles, and both of the dichlorides have the same U−Cl distance as that in $Cp^*_2UCl_2$, 2.583(6) Å. The U−F distance in $Cp^{\ddagger}_2UF_2$ is 0.5 Å shorter than the

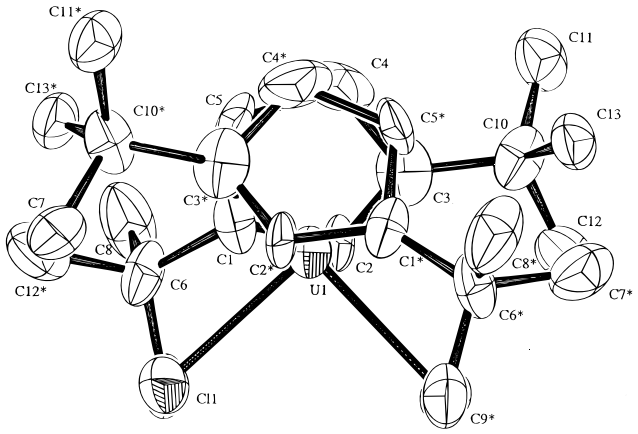

Figure 2. ORTEP drawing of $Cp^{\ddagger}_2UCl_2$ with 50% thermal ellipsoids.

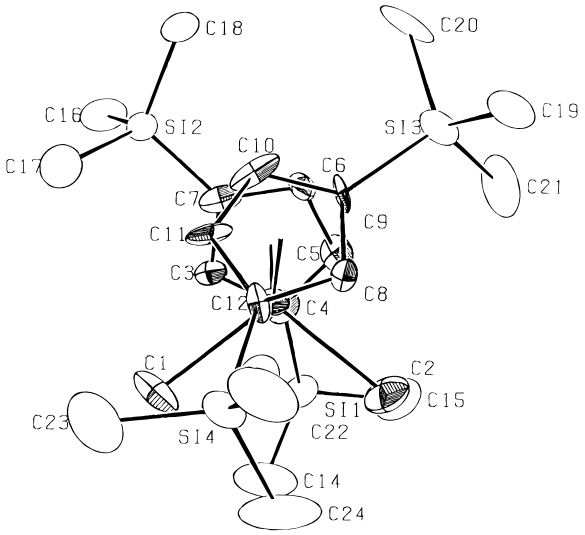

Figure 3. ORTEP drawing of Cp''_2UMe_2 with 50% thermal ellipsoids.

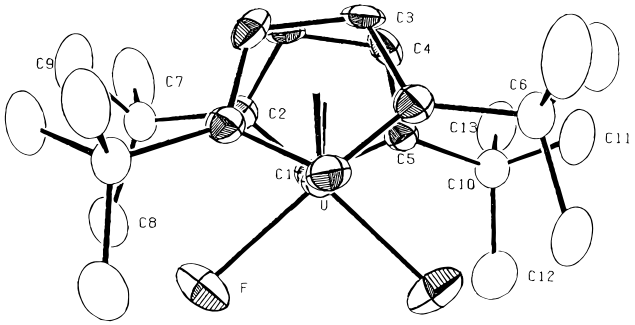

Figure 4. ORTEP drawing of $Cp^{\ddagger}_2UF_2$ with 50% thermal ellipsoids.

U−Cl distance in $Cp^{\ddagger}_2UCl_2$, in agreement with the difference between the sizes of fluoride and chloride.[20] The structure of Cp''_2UMe_2 is quite different from that of the other metallocenes. Although the idealized symmetry is C_2, the conformation of the rings is different from that in the dihalides. The Cp″ rings are staggered, with one $SiMe_3$ group on each cyclopentadienyl ring pointing between the methyl groups bonded to the uranium center. This conformation results in an opening

(20) Pauling, L. *The Nature of the Chemical Bond*; Cornell University Press: Ithaca, NY, 1960.

Table 2. Structural Parameters for Monomeric U(IV) Metallocenes[a]

	Cp''_2UCl_2	$Cp^{\ddagger}_2UCl_2$	Cp''_2UMe_2	$Cp^{\ddagger}_2UF_2$
U−X, Å	2.573(1)	2.577(4)	2.42(2)	2.086(2)
U−⟨C_{ring}⟩, Å	2.71(2)	2.77(5)	2.72(3)	2.74(3)
U−Cp, Å	2.42	2.49	2.44	2.46
Cp−U−Cp′, deg	124.7	128.1	130.8	125.3
X−U−X′, deg	95.2(2)	91.0(2)	105.0(7)	95.4

[a] Cp is the centroid of the cyclopentadienyl ring.

of the Me−U−Me angle by almost 10° relative to that found in the dihalides.

The conformations of the Cp″ or $Cp^{\ddagger}$ ligands are directly related to the radii of the X ligands in these Cp_2UX_2 complexes, which have an idealized C_{2v} structure when X is F, Cl, or Br and a C_2 structure when X is I or Me.[19] The van der Waals radii of F, Cl, Br, I, and Me are 1.35, 1.8, 1.95, 2.15, and 2.0 Å, respectively.[20] The role of the radius of X is shown by the trend in the close contacts between the X ligand and the methyl carbons of the $SiMe_3$ or CMe_3 groups; the smaller the ligand, the shorter the closest contact distance. For $Cp^{\ddagger}_2UF_2$, the closest F···CH_3C distance is 3.28 Å. The analogous Cl···CH_3C contact distance is larger in $Cp^{\ddagger}_2UCl_2$ at 3.60 Å, while the shortest Cl···CH_3Si distance in Cp''_2UCl_2 is 3.71 Å. When the C_2 structure is adopted rather than the C_{2v} structure, the H_3C···CH_3Si distance in Cp''_2UMe_2 is increased to 3.82 Å in accord with the larger radius of CH_3.

A similar explanation can account for the observed geometry of $[1,2\text{-}(Me_3C)_2C_5H_3]_2MX_2$, which adopts a C_2 geometry.[21] Since the Cl ligands of $[1,2\text{-}(Me_3C)_2C_5H_3]_2UCl_2$ would lie directly under the Me_3C groups if this molecule adopted the C_{2v} geometry of Cp''_2UCl_2 or $Cp^{\ddagger}_2UCl_2$, $[1,2\text{-}(Me_3C)_2C_5H_3]_2UCl_2$ adopts the C_2 geometry of Cp''_2UMe_2 in which the $SiMe_3$ groups of each Cp″ ligand straddle the CH_3 ligands. It is worth noting that monomeric $[1,2\text{-}(Me_3C)_2C_5H_3]_2MX$ complexes should adopt the eclipsed C_{2v} geometry, since the loss of one of the Cl ligands would remove the unfavorable interactions with the CMe_3 groups which force $[1,2\text{-}(Me_3C)_2C_5H_3]_2MX_2$ to adopt the C_2 geometry.

While it appears that the C_{2v} geometry is preferred due to the minimization of the steric interactions between the Cp ring and the $SiMe_3$ or CMe_3 group, this cannot be the only reason that this geometry is preferred. In $Cp^{\ddagger}_2UF_2$, the closest Cp···CH_3C contact is 4.30 Å. In $Cp^{\ddagger}_2UCl_2$ and Cp''_2UCl_2, the closest analogous distances are 3.69 and 3.87 Å, respectively. In Cp''_2UMe_2, the closest Cp···Me_3Si contact between Cp" rings is 3.83 Å. In comparing the structures of Cp''_2UCl_2 and Cp''_2UMe_2, the Cp···CH_3Si distances are similar although the Cl···CH_3Si distance is shorter than the H_3C···CH_3Si distance. If only intramolecular steric interactions were important, both complexes should have the same C_2 geometry, but they do not.

In addition to intramolecular steric interactions, crystal packing, and therefore intermolecular effects, appears to be important in determining the geometry of the ligands in these complexes. As shown in Figure 5, Cp''_2UCl_2 packs such that the metallocenes are "head to tail" with adjacent chains of metallocenes running

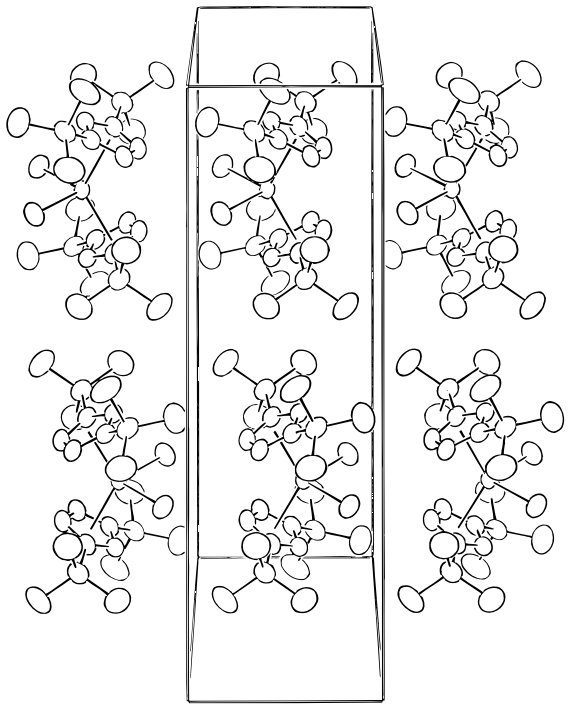

Figure 5. Packing diagram of Cp''_2UCl_2 showing the "head to tail" packing of the Cp''_2UCl_2 molecules.

in opposite directions presumably to maximize the interactions between their molecular dipoles. The spacing between the metallocenes is the *b*-axis length. Note that in $Cp^{\ddagger}_2UF_2$ the uranium atoms are 6.30 Å apart, versus 6.89 Å in $Cp^{\ddagger}_2UCl_2$. Presumably the greater dipole−dipole interaction in solid $Cp^{\ddagger}_2UF_2$ is responsible for its greatly decreased solubility in aliphatic hydrocarbon solvents. Therefore, crystal packing forces rather than intramolecular steric considerations appear to be responsible for the preference for the C_{2v} geometry, particularly when X is small. When X is large, the complexes adopt the C_2 geometry to minimize steric interactions between X and the $SiMe_3$ or CMe_3 groups. In solution, the intermolecular forces are presumably very small and therefore ligand size and electronic effects dominate the molecular properties.

While the previous complexes all have the typical bent metallocene structure, the crystal structure of $[Cp''_2UF_2]_2$ is different, since it is a centrosymmetric dimer, as shown in Figure 6. Distances and angles in $[Cp''_2UF_2]_2$ are given in Table 3. The structure of $[Cp''_2UF_2]_2$ is strongly reminiscent of the structures of $[(MeCp)_2ZrH(\mu\text{-}H)]_2$[22] and the $(Cp_2WH)_2(\mu\text{-}H)$ cation.[23] The Cp″rings and $SiMe_3$ groups on each metallocene fragment are staggered such that one Cp″ group points to the front of the metallocene wedge and one points to the rear, giving the complex idealized C_i symmetry. The terminal U−F distance is similar to that found in $Cp^{\ddagger}_2UF_2$, and the bridging U−F distances are longer at 2.30 and 2.34 Å. The U···U distance is 3.95 Å, shorter than that in $[Cp''_2UX]_2$, where X is Cl or Br.[14] Cp''_2UF_2 is able to dimerize due to the small radius of F. Since F is small, three fluoride ligands can coordinate to the uranium center while three chloride, bromide, or iodide ligands

(21) Hughes, R. P.; Lomprey, J. R.; Rheingold, A. L.; Haggerty, B. S.; Yap, G. P. A. *J. Organomet. Chem.*, **1996**, *517*, 89.

(22) Jones, S. B.; Petersen, J. L. *Inorg. Chem.* **1981**, *20*, 2889.

(23) Klingler, R. J.; Huffman, J. C.; Kochi, J. K. *J. Am. Chem. Soc.* **1980**, *102*, 208.

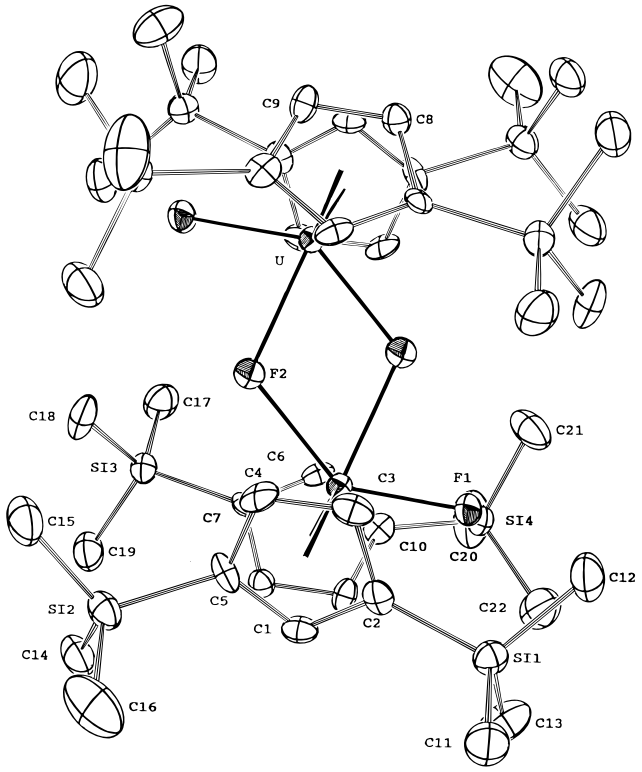

Figure 6. ORTEP drawing of $[Cp''_2UF_2]_2$ with 50% thermal ellipsoids.

Table 3. Distances (Å) and Angles (deg) in $[Cp''_2UF_2]_2$[a]

U−F1	2.073(5)	U−Cp1	2.48
U−F2	2.297(5)	U−Cp2	2.47
U−F2′	2.343(5)	U−U	3.950(1)
U-⟨C_{ring}⟩	2.76(4)		
F1−U−F2	75.6(2)	Cp1−U−Cp2	126.3
F1−U−F2′	138.9(2)	U−F2−U′	116.7(2)
F2−U−F2′	63.3(2)		

[a] Cp1 and Cp2 are the centroids of the two crystallographically independent cyclopentadienyl rings.

would presumably occupy too great a volume. Since the dimeric nature of Cp''_2UF_2 may play a role in the difference in the NMR spectrum of this complex relative to that of the other Cp''_2UX_2 complexes, the variable-temperature NMR study of these molecules was initiated to study the dynamics of these complexes in solution.

Variable-Temperature NMR Spectroscopy. While $[Cp''_2UF_2]_2$ is dimeric in the solid state, its degree of association in solution is unknown. To explore the solution constitution of these metallocenes, their variable-temperature NMR behavior was examined. Plots of δ versus $1/T$ for $[Cp''_2UF_2]_2$ and $Cp^{\ddagger}_2UF_2$ are shown in Figure 7 and reveal that the variable-temperature behaviors of these two difluoride metallocenes are very different. For $[Cp''_2UF_2]_2$, the ring a_2- and b-protons broaden and disappear at ca. −30 °C and do not reappear. The Me_3Si resonances, however, decoalesce at ca. −40 °C to give four equal-area resonances. This is the expected slow exchange pattern for a dimeric molecule with inversion symmetry as found in the solid-state structure (Figure 6). In order for the monomer to have all of its Me_3Si groups inequivalent, it must be asymmetric, a condition we have not observed among

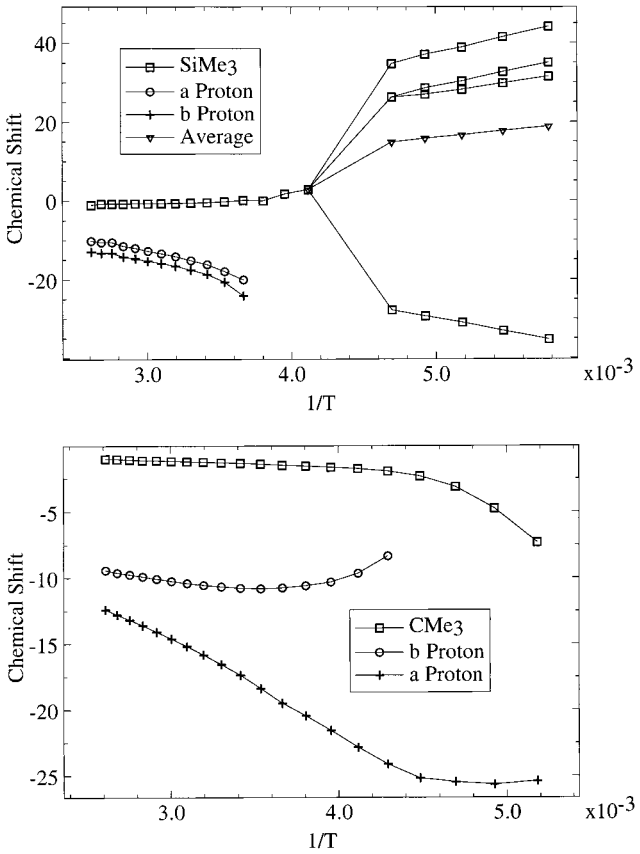

Figure 7. Plots of δ versus $1/T$ for $[Cp''_2UF_2]_2$ (a, top) and $Cp^{\ddagger}_2UF_2$ (b, bottom).

the type of disubstituted cyclopentadienyl compounds described in this paper. They all have C_2 or higher symmetry in the solid state, and the predominance of an isomer of lower symmetry in solution is unlikely. This deduction is supported by the observation that the averaged chemical shifts of the Me_3Si groups below the coalescence temperature is different from the observed chemical shift above the coalescence temperature (see Figure 7a). This disagreement shows that the Curie−Weiss law is not obeyed and that some temperature-dependent process (or processes) is operating in solution. The temperature dependence of the NMR chemical shifts of monomeric $Cp^{\ddagger}_2UF_2$ is shown in Figure 7b. Since the solid-state structure of this molecule has C_2 symmetry, two Me_3C resonances are expected at low temperature, and two broad resonances are observed at −100 °C. These resonances coalesce by −90 °C, but, as in $[Cp''_2UF_2]_2$, the δ vs $1/T$ plots are again nonlinear. One explanation of these observations is that, in solution, a rapid equilibrium between monomers and dimers exists for both complexes. Since the ratio of monomer to dimer changes with temperature, the chemical shifts of the protons will be nonlinear in $1/T$. Similar behavior observed in the variable-temperature NMR spectra of Cp_3UF was also attributed to the presence of a monomer−dimer equilibrium.[24] Further, this type of metallocene dimer is likely to be a model for the transition state that is involved in the halide exchange between metallocenes Cp_2UX_2 and Cp_2UY_2 to give two $Cp_2U(X)(Y)$ species.

(24) Fischer, R. D.; von Ammon, R.; Kanellakopolos, B. *J. Organomet. Chem.* **1970**, *25*, 123.

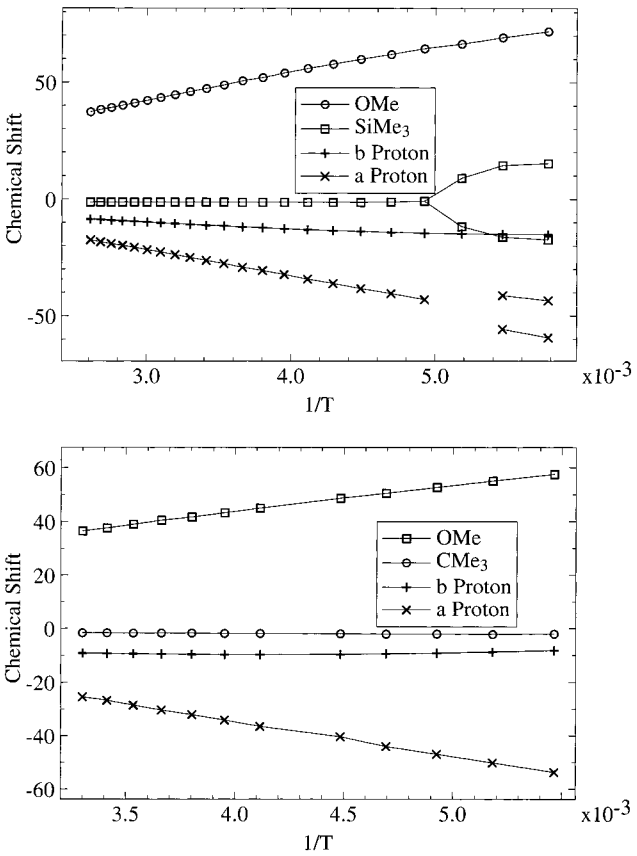

Figure 8. Plots of δ versus $1/T$ for $Cp''_2U(OMe)_2$ (a, top) and $Cp^{\ddagger}_2U(OMe)_2$ (b, bottom).

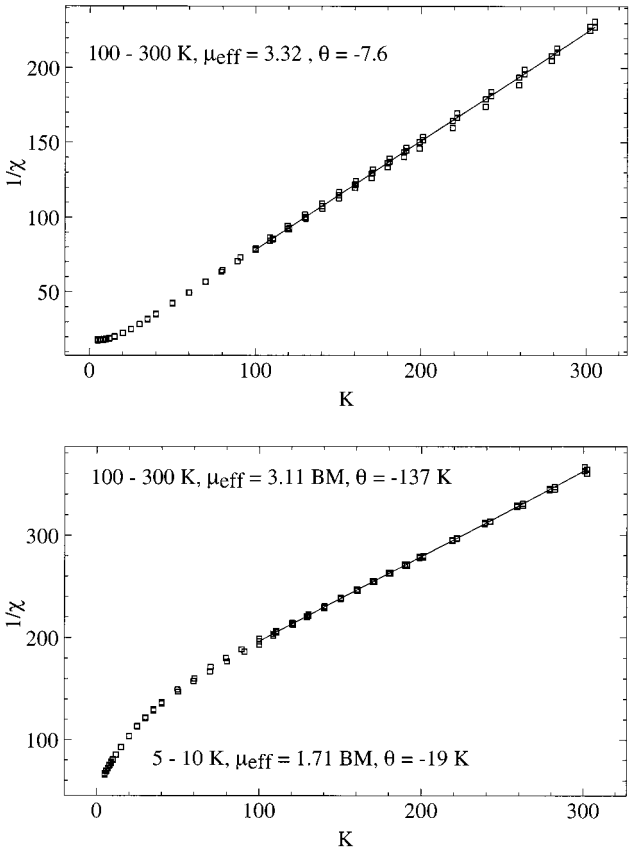

Figure 9. Plots of χ versus $1/T$ for $Cp^{\ddagger}_2UCl_2$ (a, top) and $Cp^{\ddagger}_2UF_2$ (b, bottom).

The variable-temperature behavior of $Cp^{\ddagger}_2U(OMe)_2$ was also studied. The plots of δ vs $1/T$ are linear to −100 °C, where the lines begin to broaden. Thus, above −100 °C, all of the resonances follow Curie−Weiss behavior, and no temperature-dependent equilibria need to be postulated. Presumably, the broadening is due to a decoalescence of the ring Me_3C resonances into two resonances in a molecule of C_2 symmetry. The behavior of $Cp''_2U(OMe)_2$ is similar, except that the Me_3Si resonances follow Curie−Weiss behavior to −70 °C, where they decoalesce into two equal-area resonances (Figure 8). At temperatures greater that T_c, all of the resonances follow Curie−Weiss law. Unlike the difluorides, the chemical shifts of the protons of the dimethoxides display Curie−Weiss behavior, which implies that no monomer−dimer equilibrium is present in these complexes. At low temperature, the resonances of the a_2-protons and the $SiMe_3$ groups decoalesce, each forming two new resonances; however, the resonances of the b-proton and OMe group remain sharp. Since the molecule cannot have inversion symmetry and since no single mirror plane can make both of the b-protons and the OMe groups equivalent, the complex presumably has the same C_2 structure as Cp''_2UMe_2. The barriers to site exchange calculated using the $SiMe_3$ and a_2-protons are 8.5 and 8.6 kcal/mol, respectively. Since the difluorides and dimethoxides have similar NMR spectra at room temperature but have very different geometric structures, it is unlikely that the molecular structures of the complexes are responsible for the change in NMR spectra versus the complexes of the heavier dihalides.

Solid-State Magnetic Susceptibility. Since the likelihood of a difference in molecular structure resulting in different NMR spectra for these complexes seemed small, the variable-temperature magnetic susceptibility of these complexes was examined to determine whether the complexes had similar electronic structures in the solid state. Plots of $1/\chi$ versus T for $Cp^{\ddagger}_2UCl_2$ and $Cp^{\ddagger}_2UF_2$ are shown in Figure 9. The electronic ground states of the complexes are different. In $Cp^{\ddagger}_2UCl_2$, the susceptibility is temperature-independent at low temperature, typical of a U(IV) complex with low symmetry, since no degeneracy remains among the electronic states. Surprisingly, the low-temperature susceptibility of $Cp^{\ddagger}_2UF_2$ is not temperature independent, which suggests that the two lowest lying states are coincidentally degenerate or very nearly so. At higher temperatures, $Cp^{\ddagger}_2UF_2$ has a slightly lower magnetic moment than $Cp^{\ddagger}_2UCl_2$, again supporting the premise that the electronic structures of the complexes are not the same. Since the electronic structures of the complexes are different, the dipolar contributions to the chemical shifts of the protons of the complexes are also different, and the complexes will have different NMR spectra. Presumably, all of the complexes possessing ligands that are strong π-donors have electronic structures similar to $Cp^{\ddagger}_2UF_2$ and this similarity is responsible for their similar solution chemical shift behavior. Due to the low symmetry of the complexes, their electronic structures were not further examined.

Conclusion. The syntheses of several U(IV) metallocene complexes have been described. Complexes with ligands that are strong π-donors have different NMR spectra from those with poor π-donor ligands. Some of these complexes have been crystallographically characterized. The conformations of the Cp rings in the

complexes differ, and the source of the differences is discussed. One of the complexes, $[Cp''_2UF]_2$, is a dimer. Variable-temperature NMR spectroscopy suggests that a monomer−dimer equilibrium is present in the difluorides. Variable-temperature magnetic susceptibility shows that the electronic structures of $Cp^{\ddagger}_2UCl_2$ and $Cp^{\ddagger}_2UF_2$ are different, which is thought to be responsible for the difference observed in the NMR spectra of these complexes.

Experimental Details

All reactions and manipulations were carried out in an inert atmosphere using standard Schlenk and drybox techniques. Hexane, diethyl ether, and tetrahydrofuran were dried over sodium benzophenone ketyl, distilled, and degassed immediately prior to use. Toluene, methylcyclohexane, and deuterated NMR solvents were dried over and distilled from potassium or sodium. Me_3SiBr and Me_3SiI were distilled under argon and stored over copper powder before using.

Infrared spectra were recorded on a Perkin-Elmer 283 spectrometer as Nujol mulls between CsI plates. ^{1}H NMR spectra were measured on a JEOL FX-90Q FT NMR spectrometer operating at 89.56 MHz. Chemical shifts were referenced to tetramethylsilane (δ 0), with positive values at lower field. Unless otherwise noted, all spectra were acquired at 30 °C in C_6D_6, and the chemical shifts are listed in Table 1. Melting points were measured on a Thomas-Hoover melting point apparatus in sealed capillaries and are uncorrected. Susceptibility measurements were carried out on a SHE Model 500 SQUID susceptometer. Electron impact mass spectra were recorded by the mass spectroscopy laboratory, and elemental analyses were performed by the analytical laboratories, both at the University of California, Berkeley. Numerical modeling of susceptibilities was done using the program Horizon.

The compounds Cp''_2UCl_2, Cp''_2UBr_2, and Cp''_2UI_2 have been reported previously.[15] Our syntheses are somewhat different and so are reported here. $Cp''_2U(NMe_2)_2$ has been reported, but with no experimental details or characterization.[19]

$Cp^{\ddagger}$K. Potassium (4.6 g, 120 mmol) was washed with hexane, cut into little pieces, and dried under vacuum in a 500 mL Schlenk flask. Tetrahydrofuran (150 mL) was added, and $Cp^{\ddagger}H$[25] (20 mL, 16.6 g, 93 mmol) was added by syringe. The reaction is slow. The mixture was stirred, and the flask was periodically vented to the Schlenk line. After 7 days, gas was no longer evolved, and the tetrahydrofuran was removed under reduced pressure. The remaining light pink solid was dried under vacuum. The flask was taken into the drybox, and the remaining potassium was physically removed from the powder (18.9 g, 94%). The compound was used without further characterization. The compound is insoluble in all common solvents except for hot tetrahydrofuran, in which it partially decomposes.

$Cp^{\ddagger}_2$Mg. $Cp^{\ddagger}H$[25] (18.8 mL, 15.6 g, 87.3 mmol) was added by syringe to a stirred solution of Bu_2Mg (60 mL, 0.64 M in heptane, 38.4 mmol). The solution became slightly cloudy and was heated to reflux for 3 days. The solution was cooled and then was filtered. Cooling the filtrate to −80 °C for 7 days produced colorless crystals (11.8 g, 81%). ^{1}H NMR (C_6D_6): δ 5.90 (m, 3H, ring protons), 1.31(s, 18H, CMe_3). The compound was used without further characterization.

$Cp^{\ddagger}_2UCl_2$. (a) A mixture of $KCp^{\ddagger}$ (5.25 g, 23.1 mmol) and UCl_4 (4.60 g, 11.6 mmol) was suspended in 100 mL of tetrahydrofuran. The reaction mixture immediately turned deep red and became hot. After the mixture was stirred for 8 h, the tetrahydrofuran was removed under reduced pressure. The solid residue was suspended in 150 mL of diethyl ether and filtered. The volume of the filtrate was reduced to ca. 20 mL, and the mixture was heated to redissolve the solid. Cooling to −20 °C produced large, blood red prisms (7.5 g, 93%). Mp: 165−167 °C. IR: 3070 (w), 3060 (w), 1270 (w), 1258 (w), 1248 (w), 1200 (w), 1165 (w), 1162 (w), 1050 (w), 1020 (w), 922 (w), 833 (w), 792 (w), 775 (w), 670 (w), 664 (w), 470 (w), 355 (w), 280 (w) cm^{-1}. MS (M^+) *m*/*z* (calcd, found): 662 (100, 100), 663 (30, 61), 664 (68, 66), 665 (19, 21), 666 (13, 11). Anal. Calcd for $C_{26}H_{42}Cl_2U$: C, 47.1; H, 6.33; Cl, 10.7. Found: C, 47.1; H, 6.45; Cl, 10.7.

(b) A mixture of $Cp^{\ddagger}_2Mg$ (5.00 g, 13.2 mmol) and UCl_4 (6.26 g, 16.5 mmol) was suspended in 200 mL of diethyl ether. The solution slowly turned cherry red. After 2 days of stirring, the solvent was removed under reduced pressure. The red solid residue was suspended in 200 mL of hexane, and the mixture was heated to 70 °C and then allowed to settle. The red solution was filtered, and the volume of the filtrate was reduced to 40 mL. The solution was heated to 70 °C to redissolve the solid. Cooling to −20 °C produced bright red needles (4.77 g, 50%, based upon $Cp^{\ddagger}_2Mg$). The ^{1}H NMR spectrum was identical with that of the product of route a.

Cp''_2UCl_2.[15] A mixture of UCl_4 (2.54 g, 6.68 mmol) and Cp''_2Mg[16] (2.96 g, 6.68 mmol) was suspended in 100 mL of diethyl ether. The reaction mixture slowly turned orange. After the mixture was stirred for 3 days, the diethyl ether was removed under reduced pressure, and the orange solid residue was suspended in 150 mL of hexane. The orange solution was filtered, and the volume of the solution was reduced to ca. 30 mL. The solution was heated to redissolve the solid, and slow cooling to −80 °C gave orange needles (3.3 g, 68%). The ^{1}H NMR spectrum agrees with that reported previously.[15] (Note: this reaction does not work in tetrahydrofuran presumably due to the formation of $Cp"UCl_3(thf)_2$.)

$Cp^{\ddagger}_2UBr_2$. $Cp^{\ddagger}_2UCl_2$ (0.50 g, 0.75 mmol) was dissolved in 50 mL of hexane, and Me_3SiBr (0.49 g, 3.0 mmol) was added using a syringe. The solution was stirred for 12 h, and then the volume was reduced to ca. 5 mL. Cooling to −80 °C produced red blocks (0.52 g, 91%). Mp: 185−187 °C. IR: 3110 (w), 3081 (w), 2721 (w), 1290 (w), 1249 (w), 1205 (m), 1195 (m), 1167 (s), 1058 (m), 1029 (w), 1024 (w), 938 (m), 930 (w), 864 (m), 844 (s), 780 (s), 734 (w), 722 (w) cm^{-1}. MS (M^+) *m*/*z* (calcd, found): 750 (50, 87), 751 (15, 49), 752 (100, 100), 753 (29, 72), 754 (52, 89), 755 (14, 43). Anal. Calcd for $C_{26}H_{42}Br_2U$: C, 41.5; H, 5.63. Found: C, 41.9; H: 5.69. (Note: the product often needed a second treatment with Me_3SiBr to completely metathesize all of the chlorides.) The NMR spectrum of the impurity, $Cp^{\ddagger}_2U(Br)(Cl)$, is distinct from the spectrum of $Cp^{\ddagger}_2UBr_2$ and $Cp^{\ddagger}_2UCl_2$. In all cases, the mixed halide complex is clearly visible in the NMR spectrum when the metathesis is incomplete.

$Cp"_2UBr_2$.[15] Cp''_2UCl_2[15] (2.00 g, 2.75 mmol) was dissolved in 50 mL of diethyl ether, giving an orange-green solution. Me_3SiBr (1.1 mL, 1.3 g, 8.4 mmol) was added using a syringe. The solution slowly darkened. After the mixture was stirred for 10 h, the volatile components were removed under reduced pressure. The orange solid residue was dissolved in 50 mL of hexane, giving a purple-red solution, which was then filtered. The volume of the filtrate was reduced to ca. 25 mL, and the solution was heated to dissolve the solid. Cooling to −20 °C produced bright orange needles (1.85 g, 82%). The ^{1}H NMR spectrum agrees with that reported previously.[15] (Note: the product often needed a second treatment with Me_3SiBr to completely metathesize all of the chlorides. This reaction does not work in hexane.)

$Cp^{\ddagger}_2UI_2$. $Cp^{\ddagger}_2UCl_2$ (1.5 g, 2.3 mmol) was dissolved in 50 mL of diethyl ether, and Me_3SiI (0.92 mL, 1.4 g, 6.8 mmol) was added using a syringe. The initially red solution became purple. After the mixture was stirred for 3 days, the ether was removed under reduced pressure, and the dark solid residue was dissolved in 75 mL of hexane. The solution was filtered, and the volume of the filtrate was reduced to ca. 45 mL.

(25) Venier, C. G.; Casserly, E. W. *J. Am. Chem. Soc.* **1990**, *112*, 2808−2809.

Cooling to −20 °C yielded purple-orange needles (1.52 g, 80%). Mp: 180−186 °C. IR: 3062 (w), 2722 (w), 1247 (s), 1198 (w), 1167 (m), 1076 (s), 1057 (w), 1025 (m), 847 (s), 788 (s) cm^{-1}. MS $(M)^+$ *m/z* (calcd, found): 846 (100, 100), 847 (30, 31). Anal. Calcd for $C_{26}H_{42}I_2U$: C, 36.9; H, 5.00. Found: C, 36.9; H, 5.14. (Note: the product often needed a second treatment with Me_3SiI to completely metathesize all of the chlorides.)

Cp''_2UI_2.[15] Cp''_2UCl_2[15] (1.5 g, 2.1 mmol) was dissolved in 50 mL of hexane, and Me_3SiI (0.84 mL, 1.2 g, 6.2 mmol) was added by syringe. The initially orange solution quickly turned red. After the mixture was stirred for 10 h, the volatile components were removed under reduced pressure, and the dark red solid residue was dissolved in 75 mL of hexane. The solution was filtered, and the volume of the filtrate was reduced to ca. 45 mL. Cooling to −20 °C gave purple-brown blocks (1.52 g, 81%). The ^1H NMR spectrum agrees with that reported previously.[15] (Note: the product often needed a second treatment with Me_3SiI to completely metathesize all of the chlorides.)

$Cp^{\ddagger}_2UF_2$. (a) $Cp^{\ddagger}_2UMe_2$ (1.23 g, 2.00 mmol) was dissolved in 30 mL of diethyl ether, and $BF_3{\cdot}OEt_2$ (0.51 mL, 0.59 g, 4.1 mmol) was added using a syringe. The solution immediately became warm and turned green. After 12 h, the diethyl ether was removed under reduced pressure, and the tube was heated to 80 °C under vacuum for 1 h to remove $MeBF_2$. The orange solid residue was dissolved in 50 mL of hexane, and the solution was filtered. The volume of the filtrate was reduced to ca. 25 mL. Cooling to −20 °C produced orange-yellow needles (1.00 g, 80%). Mp: 173−176 °C. IR: 3100 (w), 2730 (w), 1290 (w), 1255 (s), 1205 (m), 1165 (m), 1060 (m), 1035 (w), 925 (m), 825 (m), 820 (s), 785 (m), 725 (w), 685 (m), 665 (m), 510 (s), 480 (s), 430 (w), 355 (m), 245 (m) cm^{-1}. MS $(M)^+$ *m/z:* 630. Anal. Calcd for $C_{26}H_{42}F_2U$: C, 49.5; H, 6.71. Found: C, 49.5; H, 6.86.

(b) $Cp^{\ddagger}_2U(OMe)_2$ (1.53 g, 2.34 mmol) was dissolved in 25 mL of diethyl ether, and $BF_3{\cdot}OEt_2$ (0.60 mL, 0.70 g, 4.9 mmol) was added using a syringe. The color of the solution immediately changed from green to red. After the mixture was stirred for 6 h, the ether was removed under reduced pressure, and the tube was heated to 70 °C under vacuum for 1 h. The red solid residue was suspended in 50 mL of hexane, and the solution was filtered. The volume of the filtrate was reduced to ca. 30 mL. Cooling to −20 °C gave yellow needles (1.1 g, 74%). The ^1H NMR spectrum was identical with that of $Cp^{\ddagger}_2UF_2$ produced by route a.

$Cp^{\ddagger}_2UMe_2$. $Cp^{\ddagger}_2UCl_2$ (1.00 g, 1.51 mmol) was dissolved in 50 mL of ether, and MeLi (4.2 mL, 0.72 M in diethyl ether, 3.0 mmol) was added by syringe. The solution immediately turned orange and cloudy. After the mixture was stirred for 1 h, the ether was removed under reduced pressure. The dark orange solid residue was suspended in 25 mL of hexane, and the solution was filtered, giving a deep orange solution. The volume of the solution was reduced to ca. 2 mL. Cooling to −20 °C gave orange-brown blocks (0.73 g, 78%). Mp: 120−125 °C. IR: 1250 (s), 1200 (m), 1165 (m), 1110 (s), 1055 (m), 1025 (m), 935 (m), 845 (m), 825 (s), 810 (m), 765 (s), 675 (m), 655 (m), 405 (m) cm^{-1}. MS $(M - CH_3)^+$ *m/z*: 659. Anal. Calcd for $C_{28}H_{48}U$: C, 54.0, H, 7.71. Found C, 53.7; H, 7.83.

$[Cp''_2UF_2]_2$. $Cp''_2U(NMe_2)_2$ (0.50 g, 0.67 mmol) was dissolved in 25 mL of diethyl ether, and $BF_3{\cdot}OEt_2$ (0.17 mL, 0.19 g, 1.3 mmol) was added using a syringe. The orange solution turned bright green after 5 min. After the mixture was stirred for 12 h, the volatile components were removed under reduced pressure, and the reaction mixture was heated to 70 °C under vacuum to remove Me_2NBF_2. The green solid residue was dissolved in 40 mL of hexane, and the solution was filtered. The volume of the solution was reduced to ca. 2 mL. Cooling to −20 °C produced green blocks (0.34 g, 72%). Mp: 114−116 °C. IR: 3041 (m), 1318 (w), 1247 (s), 1204 (m), 1079 (s), 917 (s), 839 (s), 793 (s), 753 (s), 692 (m), 637 (s), 619 (w), 515 (s), 475 (s), 370 (s), 355 (s), 310 (s), 270 (m), 245 (w) cm^{-1}. MS $(M)^+$ *m/z* (calcd, found): 694 (100, 100), 695 (45, 68), 696 (23, 33), 697 (7, 12). Anal. Calcd for $C_{22}H_{42}F_2Si_4U$: C, 38.0; H, 6.09. Found: C, 37.5; H, 6.26.

$Cp''_2U(NMe_2)_2$. Cp''_2UCl_2[15] (4.00 g, 5.50 mmol) and $LiNMe_2$ (0.57 g, 11 mmol) were suspended in 100 mL of tetrahydrofuran. The solution immediately became warm and turned dark yellow-green. After the mixture was stirred for 12 h, the tetrahydrofuran was removed under reduced pressure. The green solid residue was suspended in 90 mL of hexane, and the solution was filtered. The volume of the filtrate was reduced to ca. 10 mL. Cooling to −20 °C produced orange blocks (2.82 g, 69%). Mp: 125−127 °C. IR: 3050 (w), 2767 (s), 1317 (w), 1245 (s), 1208 (m), 1141 (s), 1122 (w), 1079 (s), 1058 (m), 919 (s), 833 (s), 779 (s), 754 (s), 689 (m), 636 (m), 616 (w) cm^{-1}. MS $(M)^+$ *m/z* (calcd, found): 744 (100, 100), 745 (50, 52), 746 (25, 26). Anal. Calcd for $C_{26}H_{54}N_2Si_4U$: C, 41.9; H, 7.30; N, 3.76. Found: C, 41.9; H, 7.33; N, 3.29.

$Cp^{\ddagger}_2U(OMe)_2$. $Cp^{\ddagger}_2UCl_2$ (3.00 g, 4.52 mmol) and KOMe (0.65 g, 9.3 mmol) were suspended in 50 mL of tetrahydrofuran. After the mixture was stirred at 70 °C for 12 h, the tetrahydrofuran was removed under reduced pressure, yielding a viscous green oil, which slowly solidified under vacuum. The green solid residue was suspended in 50 mL of hexane, and the solution was filtered. The volume of the filtrate was reduced to ca. 5 mL, and additional white solid precipitated. After 12 h the solution was filtered and the volume was reduced to ca. 2.5 mL. Cooling to −20 °C produced green blocks (2.05 g, 69%). Mp: 86−88 °C. IR: 3067 (w), 2726 (w), 1297 (w), 1251 (s), 1201 (m), 1166 (m), 1115 (s), 1093 (s), 1055 (m), 1025 (m), 975 (w), 936 (m), 822 (s), 753 (s), 723 (w), 679 (m), 657 (m) cm^{-1}. MS $(M)^+$ *m/z:* 654. Anal. Calcd for $C_{28}H_{48}O_2U$: C, 51.4; H, 7.39. Found: C, 50.3; H, 7.25.

$Cp''_2U(OMe)_2$. Cp''_2UCl_2[15] (2.00 g, 2.57 mmol) and KOMe (0.40 g, 5.6 mmol) were suspended in 50 mL of tetrahydrofuran. The mixture was heated to 70 °C and was stirred for 12 h. The mixture was filtered, the tetrahydrofuran was removed under reduced pressure, and the solid was heated to 60 °C under vacuum for 1 h. The dark solid residue was suspended in 50 mL of hexane and the suspension filtered. The volume of the solution was reduced to ca. 10 mL, and a white solid precipitated. After 12 h, the solution was filtered, and the volume of the solution was reduced to ca. 2 mL. Cooling to −20 °C produced dark purple blocks (1.65 g, 84%). Mp: 95−99 °C. IR: 3043 (w), 2812 (m), 1316 (w), 1247 (s), 1212 (w), 1113 (s), 1086 (s), 1055 (m), 920 (s), 835 (s), 781 (m), 754 (s), 689 (w), 634 (s), 620 (w) cm^{-1}. MS $(M)^+$ *m/z:* 718. Anal. Calcd for $C_{24}H_{48}O_2Si_4U$: C, 40.1; H, 6.73. Found: C, 39.7; H, 6.70.

Cp''_2UMe_2. Cp''_2UCl_2[15] (2.00 g, 2.75 mmol) was dissolved in 50 mL of diethyl ether and MeLi (10.6 mL, 0.52 M in diethyl ether, 5.5 mmol) was added by syringe. The solution immediately turned red-orange and cloudy. After the mixture was stirred for 10 h, the solvent was removed under reduced pressure. The orange solid residue was suspended in 50 mL of hexane, and the solution was filtered. The volume of the filtrate was reduced to ca. 3 mL. Cooling to −20 °C produced red-orange crystals (1.45 g, 77%). Mp: 120−125 °C. IR: 1250 (s), 1200 (m), 1165 (m), 1110 (s), 1055 (m), 1025 (m), 935 (m), 845 (m), 825 (s), 810 (m), 765 (s), 675 (m), 655 (m), 405 (m) cm^{-1}. MS $(M - CH_3)^+$ *m/z:* 659. Anal. Calcd for $C_{24}H_{48}Si_4U$: C, 54.0; H, 7.71. Found: C, 53.7; H, 7.83.

$Cp^{\ddagger}_2U(Me)Cl$. $Cp^{\ddagger}_2UCl_2$ (2.00 g, 3.01 mmol) was dissolved in 50 mL of hexane. MeLi (5.80 mL, 0.52 M in ether, 3.0 mmol) was added using a syringe. The solution immediately turned a cloudy red-orange. After the mixture was stirred for 8 h, the solution was filtered, and the volume of the solvent was reduced to ca. 7 mL. Cooling to −20 °C produced red-orange blocks (1.35 g, 70%). Mp: 128−132 °C. IR: 3091 (w), 2740 (w), 2720 (w), 1293 (w), 1248 (s), 1199 (m), 1166 (m), 1114 (m), 1056 (m), 1023 (m), 935 (m), 927 (m), 832 (s), 811 (w), 775 (s), 659 (w) cm^{-1}. MS peaks at *m/z* 607, 627, and 662 are seen, corresponding to $Cp^{\ddagger}_2UMe$, $Cp^{\ddagger}_2UCl$, and $Cp^{\ddagger}_2UCl_2$, respec-

Table 4. Crystal Data

	Cp''_2UCl_2	$Cp^{\ddagger}_2UCl_2$	Cp''_2UMe_2	$Cp^{\ddagger}_2UF_2$	$[Cp''_2UF_2]_2$
space group	*I*2/*a*	*C*2/*c*	$P2_12_12_1$	*P*2/*n*	$P2_1/n$
a, Å	22.28(1)	25.4903(6)	10.806(2)	14.155(4)	11.519(3)
b, Å	7.069(4)	6.8922(2)	16.185(8)	6.302(1)	21.892(7)
c, Å	20.558(8)	18.7124(3)	18.034(6)	14.250(5)	12.846(3)
α, deg	90	90	90	90	90
β, deg	102.03(3)	124.077(1)	90	92.46(3)	116.07(2)
γ, deg	90	90	90	90	90
V, Å^3	3166.87	2723.0(1)	3154(2)	1270	2910
Z	4	4	4	2	2
fw	680.98	663.55	687.02	630.65	1389.90
d(calcd), g/cm^3	1.428	1.618	1.448	1.65	1.586
μ(calcd), cm^{-1}	50.154	61.69	50.438	60.83	54.708
no. of rflns collected	5822	5448	2366	1930	5868
no. of unique rflns	2818	2341	2343	1684	4007
R_{int}	0.030	0.129			
no. of rflns, $F_o^2 > 3\sigma(F_o^2)$	2179	1880	2075	1415	3109
R,%	2.3	10.4	4.2	1.8	3.4
R_w,%	2.8	6.8	5.4	2.2	3.4
GOF	0.83	6.85	1.39	1.18	1.97

tively. Anal. Calcd for $C_{27}H_{45}ClU$: C, 50.4; H, 7.05. Found: C, 50.0; H, 6.84.

$Cp''_2U(Me)Cl$. Cp''_2UCl_2[15] (2.00 g, 2.75 mmol) was dissolved in 50 mL of hexane, and MeLi (2.75 mL, 1.0 M in ether, 2.8 mmol) was added by syringe. The solution immediately turned red-orange and cloudy. After the mixture was stirred for 12 h, it was filtered, and the volume of the filtrate was reduced to ca. 7 mL. The solution was heated to 70 °C to redissolve the solid. Cooling to −20 °C produced red-orange, flower-shaped crystals (1.42 g, 72%). Mp: 122−124 °C. IR: 1403 (w), 1317 (m), 1247 (s), 1202 (m), 1112 (w), 1075 (s), 1053 (w), 912 (s), 840 (s), 793 (s), 751 (s), 689 (m), 627 (m), 469 (m), 411 (w), 362 (m), 312 (m), 278 (m), 245 (w) cm^{-1}. MS peaks at *m*/*z* 671, 691, and 726 are seen corresponding to Cp''_2UMe, Cp''_2UCl, and Cp''_2UCl_2, respectively.

Susceptibility Measurements. In an argon-filled drybox, a ca. 100 mg sample was weighed into a cylindrical holder consisting of two tightly fitting Kel-F cups, which were sealed with silicone grease. The sample was quickly inserted into the instrument, a SHE model 500 SQUID susceptometer. The sample was centered, and data were obtained at 0.5 and 4.0 T from 5 to 300 K.

The data were treated as follows. First, the contribution from the container was subtracted from the raw data using data from susceptibility measurements of the container alone. The magnetization was then converted to χ_{gram} and then χ_{mol} using the mass of the sample and the molecular weight of the complex. The diamagnetic contribution of the ligands was calculated and was added to χ_{mol} to yield $\chi_{corr.}$ Effective magnetic moments were calculated by linear regression from plots of $1/\chi_{corr}$ versus *T* in Kelvin.

Crystallography. Cp''_2UCl_2. Orange needles of the compound were grown by cooling a saturated hexane solution to −30 °C. The crystals were dried under reduced pressure and loaded into quartz capillaries in an inert-atmosphere box. A crystal measuring 0.08 × 0.20 × 0.60 mm was transferred to an automated Picker FACS-1 diffractometer. The crystal was centered in the beam. Automatic peak search and indexing procedures indicated that the crystal possessed a body-centered monoclinic cell and yielded the cell parameters. The cell parameters and data collection parameters are given in Table 4.

The 5882 raw intensity data were converted to structure factor amplitudes and their esds by correction for scan speed, background, and Lorentz−polarization effects.[26] Inspection of the intensity standards showed no great change in intensity. An intensity correction varying from 1.073 to 0.982 was applied to the data. The systematic absences (*h*,0,*l*), *h* odd, and (*h*,0,*l*), *l* odd, were then rejected, and the data were averaged (R_{int} = 0.030), yielding 2818 unique data, of which 2179 had $F_o > 3\sigma(F_o)$. Azimuthal scans showed fairly flat absorption curves. No absorption correction was applied. The systematic absences indicated that the space group was *I*2/*a* or *I*2/*c*. *I*2/*a* was chosen.

The cell volume indicated that four molecules were present in the unit cell. The uranium atom had to be on a special position. Since the molecule could have C_2 symmetry, the first special position was chosen. The uranium atom position and the positions of the chlorine and silicon atoms were obtained by solving the Patterson map. Successive Fourier searches yielded the rest of the heavy-atom positions. The heavy-atom structure was refined by standard least-squares and Fourier techniques. The heavy atoms were refined anisotropically. The hydrogen atoms were located in a difference Fourier, and the hydrogen positions were then calculated on the basis of idealized bonding geometry and assigned thermal parameters equal to 5 Å^2 for the cyclopentadienyl hydrogen atoms and 10 Å^2 for the trimethylsilyl hydrogen atoms. After one least-squares cycle, the hydrogen atoms were refined isotropically. A final difference Fourier map showed no additional atoms in the asymmetric unit. Examination of intermolecular close contacts (<3.5 Å) showed that the molecule was a monomer.

The final residuals for 216 variables refined against the 2179 unique data with $F_o > 3\sigma(F_o)$ were $R = 2.3\%$, $R_w = 2.8\%$, and GOF = 0.83. The *R* value for all data (including unobserved reflections) was 4.2%. The quantity minimized by the least-squares refinements was $w(|F_o| - |F_c|)^2$, where *w* is the weight given to a particular reflection. The *p* factor, used to reduce the weight of intense reflections, was set to 0.05.[27] The analytical forms of the scattering factor tables for neutral atoms were used, and all non-hydrogen scattering factors were corrected for both the real and imaginary components of anomalous dispersion.[28] The largest positive and negative

(26) The data reduction formulas are

$$F_o^2 = \frac{\omega}{Lp}(C - 2B)$$

$$\sigma_o(F_o^2) = \frac{\omega}{Lp}(C + 4B)^{1/2}$$

$$F_o = (F_o^2)^{1/2}$$

$$\omega_o(F) = [F_o^2 + \sigma_o(F_o^2)]^{1/2} - F_o$$

where *C* is the total count of the scan, *B* is the sum of the two background counts, *ω* is the scan speed used in deg/min, and

$$\frac{1}{Lp} = \frac{(\sin 2\theta)(1 + \cos^2 2\theta_m)}{1 + \cos^2 2\theta_m - \sin^2 2\theta}$$

is the correction for Lorentz and polarization effects for a reflection with scattering angle 2θ and radiation monochromatized with a 50% perfect single-crystal monochromator with scattering angle $2\theta_m$.

peaks in the final difference Fourier map have electron densities of 0.51 and −0.49 e/Å^2, respectively.

$Cp^{\ddagger}_2UCl_2$. Red crystals of the compound were grown by cooling a hexane solution to −20 °C. The crystals were then placed in a Petri dish along with Paratone N in a glovebox. A plate-shaped crystal measuring 0.12 × 0.26 × 0.23 mm was mounted on the end of a 0.2 mm thin-walled quartz capillary. The crystal was transferred to an Siemens SMART diffractometer and cooled to −95 °C under a cold stream previously calibrated by a thermocouple placed in the sample position. The crystal was centered in the beam. Automatic peak search and indexing procedures indicated that the crystal possessed a *C*-centered monoclinic cell and yielded the unit cell parameters. The cell parameters and data collection parameters are given in Table 4. On the basis of a statistical analysis of intensity distribution and the successful solution and refinement of the crystal structure, the space group was found to be *C*2/*c*.

An arbitrary hemisphere of data was collected using the default parameters for the diffractometer. The data were collected as 30 s images with an area detector. Two images were averaged to give the net image data. The image data were integrated to give intensity data using the program SAINT. The 5448 raw intensity data were converted to structure factor amplitudes and their esds by correction for scan speed, background, and Lorentz−polarization effects.[26] Inspection of the intensity standards showed no decrease in intensity over the duration of data collection. An empirical absorption correction using an ellipsoidal model for the crystal was applied to the intensity data on the basis of the intensities of all intense equivalent reflections ($T_{max} = 0.979$, $T_{min} = 0.227$). Averaging equivalent reflections gave 2341 unique data ($R_{int} = 0.129$).

The uranium atom positions were obtained by direct methods. Refinement on the uranium positions followed by a difference Fourier search yielded the other heavy-atom positions. The heavy-atom structure was refined by standard least-squares and Fourier techniques. The hydrogen positions were calculated on the basis of idealized bonding geometry and assigned thermal parameters equal to 1.15 Å^2 larger than the carbon atom to which they were connected. The hydrogen positions were included in the structure factor calculations but not refined by least squares. A final difference Fourier map showed no additional atoms in the asymmetric unit. No close (<3.5 Å) intermolecular contacts were found.

The final residuals for 132 variables refined against the 1880 unique data with $I > 3\sigma(I)$ were $R = 10.4\%$, $R_w = 6.8\%$, and GOF = 6.85. The quantity minimized by the least-squares refinements was $w(|F_o| - |F_c|)^2$, where w is the weight given to a particular reflection. The p factor, used to reduce the weight of intense reflections, was set to 0.03.[27] The analytical forms of the scattering factor tables for neutral atoms were used, and all non-hydrogen scattering factors were corrected for both the real and imaginary components of anomalous dispersion.[28]

Inspection of the residuals ordered in the ranges of (sin θ)/λ, $|F_o|$, and parity and values of the individual indexes showed no trends other than the previously mentioned secondary extinction. No reflections had anomalously high values of $w\Delta^2$. The largest positive and negative peaks in the final difference Fourier map have electron densities of 6.42 and −6.01 e/Å^2, respectively.

Cp''_2UMe_2. Orange crystals of the compound were grown by cooling a saturated ether solution to −30 °C. The crystals were then placed in a small Petri dish and covered with Paratone N, a high-molecular-weight hydrocarbon oil. A block-shaped single crystal measuring 0.45 × 0.40 × 0.40 mm was mounted on the end of a 0.4 mm diameter quartz capillary. The crystal was transferred to an Enraf-Nonius CAD-4 diffractometer and cooled to −98 °C under a cold stream of nitrogen gas previously calibrated by a thermocouple placed in the sample position. The crystal was centered in the beam. Automatic peak search and indexing procedures indicated that the crystal possessed a primitive orthorhombic cell and yielded the cell parameters. The cell parameters and data collection parameters are given in Table 4.

The 2366 raw intensity data were converted to structure factor amplitudes and their esds by correction for scan speed, background, and Lorentz−polarization effects.[26] Inspection of the intensity standards showed no loss of intensity during the data collection. The 23 systematic absences (h,0,0), h odd, (0,k,0), k odd, and (0,0,l), l odd, were then rejected, yielding 2343 unique data, of which 2075 possessed $F_o > 3\sigma(F_o)$. Azimuthal scan data showed a difference of $I_{min}/I_{max} = 0.69$ for the average curve. An empirical absorption correction was applied on the basis of the average curve. The systematic absences indicated that the space group was $P2_12_12_1$.

The cell volume indicated that four molecules were present in the unit cell. The uranium atom position was obtained by solving the Patterson map. Successive Fourier searches yielded the rest of the heavy-atom positions. The heavy-atom structure was refined by standard least-squares and Fourier techniques. The heavy atoms were refined anisotropically. Hydrogen atoms were placed at calculated positions with thermal parameters 1.3 times the thermal parameters of the carbon atoms to which they were bound. At the end of the refinement, the enantiomer was changed and the structure refined. The refinement was very slightly worse, so the enantiomer was changed back to the original one, and the structure was re-refined. A final difference Fourier map showed no additional atoms in the asymmetric unit. Examination of intermolecular close contacts (<3.5 Å) showed that the molecule was a monomer.

The final residuals for 263 variables refined against the 2075 unique data with $F_o > 3\sigma(F_o)$ were $R = 4.22\%$, $R_w = 5.38\%$, and GOF = 1.39. The R value for all data (including unobserved reflections) was 5.01%. The quantity minimized by the least-squares refinements was $w(|F_o| - |F_c|)^2$, where w is the weight given to a particular reflection. The p factor, used to reduce the weight of intense reflections, was set to 0.03 initially, but later changed to 0.06.[27] The analytical forms of the scattering factor tables for neutral atoms were used, and all non-hydrogen scattering factors were corrected for both the real and imaginary components of anomalous dispersion.[28]

Inspection of the residuals ordered in the ranges of (sin θ)/λ, $|F_o|$, and parity and values of the individual indexes showed that secondary extinction was occurring. A secondary extinction coefficient was included in the refinement; its final value was 1.2×10^{-8}. One reflection had anomalously high values

(27)

$$R = \frac{\sum ||F_o| - |F_c||}{\sum |F_o|}$$

$$R_w = \left[\frac{\sum (|F_o| - |F_c|)^2}{\sum w F_o^{\,2}}\right]^{1/2}$$

$$\mathrm{GOF} = \left[\frac{\sum (|F_o| - |F_c|)^2}{(n_o - n_v)}\right]^{1/2}$$

where n_o is the number of observations and n_v is the number of variable parameters, and the weights were given by

$$w = \frac{1}{\sigma^2(F_o)}$$

$$\sigma(F_o^{\,2}) = [\sigma_o^{\,2}(F_o^{\,2}) + (pF^2)^2]^{1/2}$$

where $\sigma^2(F_o)$ is calculated as above from $\sigma(F_o^2)$ and where p is the factor used to lower the weight of intense reflections.

(28) Cromer, D. T.; Waber, J. T. In *International Tables for X-ray Crystallography*; Kynoch Press: Birmingham, England, 1974; Vol. IV.

of $w\Delta^2$ and was weighted to zero toward the end of the refinement. The largest positive and negative peaks in the final difference Fourier map have electron densities of 2.44 and -0.29 e/Å^2, respectively, and are associated with the uranium atom.

$Cp^{+}_2UF_2$. Light orange crystals of the compound were grown by cooling a hexane solution to −20 °C. The supernatant was removed using a cannula, and degassed Paratone N, a high-molecular-weight, aliphatic hydrocarbon oil was poured into the Schlenk tube. A suitable square crystal measuring 0.28 mm × 0.28 mm × 0.08 mm was mounted on the end of a 0.2 mm thin-walled glass capillary. The crystal was transferred to an Enraf-Nonius CAD-4 diffractometer and cooled to −88 °C under a cold stream previously calibrated by a thermocouple placed in the sample position. The crystal was centered in the beam. Automatic peak search and indexing procedures indicated that the crystal possessed a primitive monoclinic cell and yielded the unit cell parameters. The cell parameters and data collection parameters are given in Table 4.

Inspection of the raw data indicated that the space group contained an *n* glide plane, so the centric space group $P2/n$ was chosen. The 1930 raw intensity data were converted to structure factor amplitudes and their esds by correction for scan speed, background, and Lorentz−polarization effects.[26] Inspection of the intensity standards showed no decrease in intensity over the duration of data collection. Inspection of the azimuthal scan data showed a variation of $I_{min}/I_{max} = 0.52$ for the averaged curve. An empirical absorption correction was applied to the intensity data on the basis of the average curve. Removal of the 181 systematic absences $(h,0,l)$, $h + l$ odd, and the 68 redundant data $(+h,+k,-l)$ left 1684 unique data.

The uranium atom positions were obtained by solving the Patterson map. The uranium atom was on a special position (0.25, 0.13, 0.25) with 2-fold rotational symmetry. Refinement on the uranium positions followed by a difference Fourier search yielded the other heavy-atom positions. The heavy-atom structure was refined by standard least-squares and Fourier techniques. The heavy atoms were refined with isotropic and then anisotropic thermal parameters. The hydrogen positions were calculated on the basis of idealized bonding geometry and assigned thermal parameters equal to 1.15 Å^2 larger than the carbon atom to which they were connected. The hydrogen positions were included in the structure factor calculations but not refined by least squares. Toward the end of the refinement, examination of the extinction test listing indicated that secondary extinction was occurring. The secondary extinction coefficient was initially set to 1.7×10^{-7} and was refined to a final value of 2.67×10^{-7}. A final difference Fourier map showed no additional atoms in the asymmetric unit. No close (<3.5 Å) intermolecular contacts were found.

The final residuals for 133 variables refined against the 1415 unique data with $F_o > 3\sigma(F_o)$ were $R = 1.78\%$, $R_w = 2.20\%$, and GOF = 1.19. The *R* value for all data (including unobserved reflections) was 2.02%. The quantity minimized by the least-squares refinements was $w(|F_o| - |F_c|)^2$, where *w* is the weight given to a particular reflection. The *p* factor, used to reduce the weight of intense reflections, was set to 0.03.[27] The analytical forms of the scattering factor tables for neutral atoms were used, and all non-hydrogen scattering factors were corrected for both the real and imaginary components of anomalous dispersion.[28]

Inspection of the residuals ordered in the ranges of $(\sin\theta)/\lambda$, $|F_o|$, and parity and values of the individual indexes showed no trends other than the previously mentioned secondary extinction. No reflections had anomalously high values of $w\Delta^2$. The largest positive and negative peaks in the final difference Fourier map have electron densities of 1.02 and -0.54 e/Å^2, respectively, and are associated with the uranium atom.

$[Cp''_2UF_2]_2$. Dark green crystals of the compound were grown by heating a hexane solution to about 80 °C and then cooling slowly to room temperature. The supernatant was removed using a cannula, and degassed Paratone N, a high-molecular-weight, aliphatic hydrocarbon oil was poured into the Schlenk tube. A suitable, roughly cubic crystal measuring 0.28 × 0.30 × 0.30 mm was mounted on the end of a 0.2 mm thin-walled quartz capillary. The crystal was transferred to an Enraf-Nonius CAD-4 diffractometer and cooled to −111 °C under a cold stream previously calibrated by a thermocouple placed in the sample position. The crystal was centered in the beam. Automatic peak search and indexing procedures indicated that the crystal possessed a primitive monoclinic cell and yielded the unit cell parameters. The cell parameters and data collection parameters are given in Table 4.

The data were collected in two blocks $(+h,\pm k,+l)$ and $(+h,+k,-l)$. The 5868 raw intensity data were converted to structure factor amplitudes and their esds by correction for scan speed, background, and Lorentz−polarization effects.[26] Inspection of the intensity standards showed no decrease in intensity over the duration of data collection for the first block of data and a 5% decrease in intensity for the second block of data. The second block was then corrected for a decay of 5%. The 157 systematic absences $(0,k,0)$, *k* odd, and $(h,0,l)$, $h + l$ odd, and the 1499 redundant data $(+h,-k,+l)$ and the 195 duplicated $(h,k,0)$ data were then rejected, yielding 4007 unique data. No empirical absorption correction could be applied because a large piece of ice had grown on the glass capillary, and when the goniometer head was raised to 90° in χ, the capillary snapped off. Inspection of the collected data showed systematic absences for $(0,k,0)$, *k* odd, and $(h,0,l)$, $h + l$ odd, indicating that the space group was $P2_1/n$.

The molecule was initially believed to be a monomer with $Z = 4$. The uranium atom positions were obtained by solving the Patterson map. Refinement on the uranium positions followed by a difference Fourier search yielded the other heavy-atom positions. The heavy-atom structure was refined by standard least-squares and Fourier techniques. The heavy atoms were refined isotropically, and the hydrogen atom positions were calculated. A numerical absorption correction (DIFABS) was applied, and the heavy-atom positions were refined anisotropically with the hydrogen atoms in calculated positions. The hydrogen positions were calculated on the basis of idealized bonding geometry and assigned thermal parameters equal to 1.3 Å^2 larger than the carbon atom to which they were connected. The hydrogen positions were included in the structure factor calculations but not refined by least squares. A final difference Fourier map showed no additional atoms in the asymmetric unit. Examination of intermolecular close contacts(<3.5 Å) showed that the molecule was actually a dimer with two bridging fluoride ligands.

The final residuals for 263 variables refined against the 4007 unique data with $F_o > 3\sigma(F_o)$ were $R = 3.35\%$, $R_w = 3.58\%$, and GOF = 1.97. The *R* value for all data (including unobserved reflections) was 5.42%. The quantity minimized by the least-squares refinements was $w(|F_o| - |F_c|)^2$, where *w* is the weight given to a particular reflection. The *p* factor, used to reduce the weight of intense reflections, was set to 0.03 initially but was later changed to 0.02.[27] The analytical forms of the scattering factor tables for neutral atoms were used, and all non-hydrogen scattering factors were corrected for both the real and imaginary components of anomalous dispersion.[28]

Inspection of the residuals ordered in the ranges of $(\sin\theta)/\lambda$, $|F_o|$, and parity and values of the individual indexes showed no trends. Fourteen reflections had anomalously high values of $w\Delta^2$ and were weighted to zero toward the end of the refinement. The largest positive and negative peaks in the final difference Fourier map have electron densities of 0.93 and -0.30 e/Å^2, respectively, and are associated with the uranium atom.

Acknowledgment. We thank F. J. Hollander and A. Zalkin for help with crystallography. W.W.L. thanks the National Science Foundation for a graduate fellowship. This work was partially supported by the Director, Office of Energy Research, Office of Basic Energy Sciences, Chemical Sciences Division, of the U.S. Department of Energy under Contract No. DE-AC03-76SF00098.

Supporting Information Available: Tables giving atomic positions and anisotropic thermal parameters for Cp''_2UCl_2, $Cp^{\ddagger}_2UCl_2$, Cp''_2UMe_2, $Cp^{\ddagger}_2UF_2$, and $[Cp''_2UF_2]_2$. This material is available free of charge via the Internet at http://pubs.acs.org. Tables of structure factors are available from the authors upon request.

OM9805988